Received: 28 December 2017 | Revised: 17 April 2018 | Accepted: 28 June 2018

DOI: 10.1002/rob.21813

FIELD REPORT

WILEY

Developing and deploying a tethered robot to map extremely steep terrain

Patrick McGarey[1] | David Yoon[1] | Tim Tang[1] | François Pomerleau[2] | Timothy D. Barfoot[1]

[1]University of Toronto, Toronto, Ontario, Canada

[2]University of Laval, Quebec, Canada

Correspondence
Patrick McGarey, University of Toronto, Ontario, Canada.
Email: patrick.mcgarey@robotics.utias.utoronto.ca

Abstract

Mobile robots outfitted with a supportive tether are ideal for gaining access to extreme environments for mapping when human or remote observation is not possible. This paper is a field report covering both the development and field testing of our Tethered Robotic eXplorer (TReX) to map a steep, tree-covered rock outcrop in a gravel mine. TReX is a mobile robot designed for the purpose of mapping extremely steep and cluttered environments for geologic and infrastructure inspection. In comparison to other systems, our design improves tethered mobility by enabling rotational freedom on steep slopes using a center-pivoting tether management payload. To map the terrain, we leverage the rotation of an actuated tether spool with an attached two-dimensional (2D) lidar, which rotates to both manage tether and produce 3D scans. Given that mapping requires vehicle motion, we also evaluate two existing, real-time approaches to estimate the trajectory of the robot and rectify motion distortion from individual scans before alignment into the map: (a) a continuous-time, lidar-only approach that handles asynchronous measurements using a physically motivated, constant-velocity motion prior, and (b) a method that computes visual odometry from streaming stereo images to use as a motion estimate during scan collection. Once rectified, individual scans are matched to the global map by an efficient variant of the Iterative Closest Point (ICP) algorithm. Our results include a comparison of estimated maps and trajectories to ground truth (measured by a remote survey station), an example of mapping in highly cluttered terrain, and lessons learned from the design and deployment of TReX.

KEYWORDS

extreme environments, mapping, terrestrial robotics, tetheredrobotics, wheeled robots

1 | INTRODUCTION

We are motivated to use tethered mobile robots for mapping extreme environments not suitable for human or remote survey for the purpose of geologic and infrastructure inspection. Deploying an unmanned aerial vehicle to map a steep rock outcrop below the tree canopy would be hazardous, given the challenge of navigating cluttered environments and limited operational time imposed by on-board power storage. Alternatively, a tethered robot can leverage an attached electromechanical tether, which provides support on steep terrain, continuous off-board power supply, and a reliable wired connection to a remote base station. However, outside of underwater applications where tethering is standard, tethers are not widely used for ground robots because tether management is an unsolved problem in challenging environments (Nagatani et al., 2013). Sinden (1990) first introduced the need for tether management in complex environments

FIGURE 1 TReX field deployment: Our tethered mobile robot navigates extremely steep terrain to generate a 3D map of a spanning rock outcrop that is partially occluded by vegetation. The experiment, which was conducted over several days in an open-pit mine in Northern Ontario, Canada, involved just over 1 km of driving on extremely steep terrain. TReX is anchored at the top of the cliff and manually piloted. The attached electromechanical tether (bright green) provides support, off-board power, and wired communications between the robot and base station [Color figure can be viewed at wileyonlinelibrary.com]

as a means to prevent entanglement. Since then, a variety of tethered robots have been developed and tested on steep terrain, but a lack of demonstrated autonomy and mobility has slowed both interest and progress in tethered systems. We have developed a tethered platform specifically to address these problems to more efficiently map extremely steep terrain.

In this field report, we detail the system design of TReX (originally introduced in McGarey, Pomerleau, and Barfoot (2015), draw comparisons to prior tethered systems, and evaluate the system in a field deployment to an open-pit gravel mine, where the robot was piloted on steep, cluttered terrain to map exposed bed rock as shown in Figure 1. Mapping relies on a two-dimensional (2D) lidar mounted to a rotating tether spool to produce scans of the environment as TReX drives and deploys tether. To produce 3D maps from the field deployment, we account for motion distortion using two existing approaches to estimate the robot's trajectory and handle motion-distorted scans using (a) a continuous-time approach that accounts for asynchronous lidar measurements with a physically motivated motion prior, and (b) an approach that uses visual odometry (VO) to estimate the motion of the robot during the collection of a single 3D scan. Both approaches, originally described in McGarey, Tang, Yoon, Pomerleau, and Barfoot (2017) attempt to reduce distortion before scan alignment, which is handled by an implementation of the Iterative Closest Point (ICP) algorithm. We compare estimated maps and trajectories with ground truth collected by a Leica Total Station, which produces an undistorted point cloud of nonoccluded terrain and tracks the position of a marker attached to the robot if visible. Our field results show that the odometry-aided approach is best suited for mapping highly unstructured environments when the robot's motion is complex. We also provide evidence that tethered robots are well suited for mapping steep, occluded environments by highlighting an example map collected in an area hidden from remote view by vegetation. We conclude with a discussion of lessons learned from the development and deployment of TReX.

The paper is structured as follows: Section 2 gives a brief history of tethered robots and some background on lidar-based mapping, Section 3 details the TReX systems design, Section 4 describes our mapping approach, Section 5 summarizes the field deployment and provides mapping results, Section 6 outlines lessons learned, and Section 7 offers concluding remarks and future extensions.

2 | RELATED WORK

2.1 | Tethered robots

Tethered robots can be used to explore extreme areas considered dangerous or time consuming for human exploration (e.g., field geology, emergency response, and infrastructure inspection). Tethered mobile robots have been successfully used to explore steep terrain for geologic inspection in the past. Dante I and II (shown in Figure 2) were the first tethered climbing systems to be designed and deployed in extreme terrain (Wettergreen, Thorpe, & Whittaker, 1993). Their unique, eight-legged "walking" configuration allowed for traversing steep, snow-covered volcanic craters and, through testing, demonstrated the challenges of tethered mobility for the first time. During several field deployments, issues related to mobility under tension and tether management resulted in extensive damage to the platform. Following Dante, TRESSA leveraged a conventional, wheeled rover with a pair of tethers to explore steep slopes (Huntsberger et al., 2007). The dual-tether system provided additional stability, yet made tether management inherently more complex. In fact, tether deployment was coordinated by two separate anchor robots located at the top of a cliff. Additionally, by not managing tether on board, the cables were exposed to abrasion due to dragging, which in turn, decreased the effective range of the robot. More recently, Matthews and Nesnas (2012) developed the Axel robot, which returns to the idea of on-board tether management and uses a novel dual-wheel, self-righting design as shown in image (3) of Figure 2.

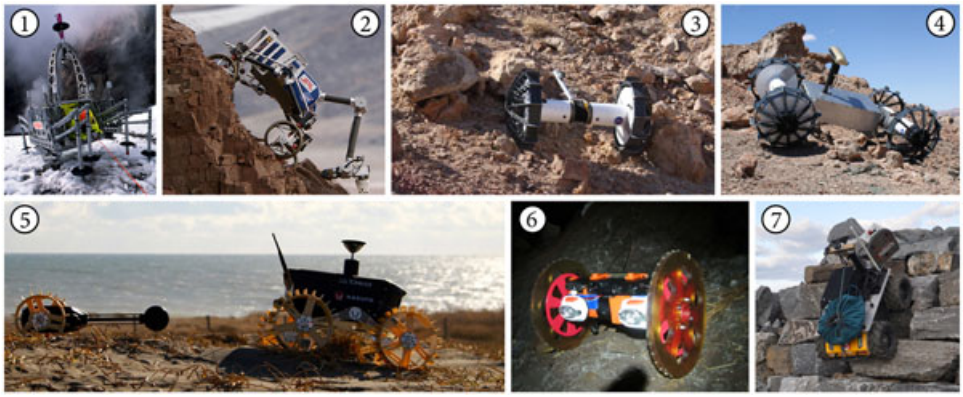

FIGURE 2 Review of tethered robots: (1) Dante II (Bares & Wettergreen, 1999), (2) TRESSA (Huntsberger et al., 2007), (3) Axel II and (4) DuAxel (Matthews & Nesnas, 2012), (5) Tetris and Moonraker (Britton et al., 2015), (6) VolcanoBot (JPL/CalTech), and (7) vScout (Stenning et al., 2015) [Color figure can be viewed at wileyonlinelibrary.com]

Image (4) shows a variation of the design, which uses two Axel robots to construct a redundant four-wheeled platform, where one of the Axel robots serves as the "anchor" while the other descends to explore. Axel's design has inspired the Moonraker and Tetris robots (a lunar rover concept from Tohoku University), and VolcanoBot (a volcanic vent mapping prototype from JPL/Caltech), which are shown in images (5) and (6). The key issue with Axel is that the potential for embedding mapping sensors is limited by design; the current system has a forward-looking stereo camera centered between the wheels with limited space for additional sensors. With the idea that conventional rover platforms are better equipped for sensor integration, the vScout prototype was developed as a precursor to TReX (Stenning et al., 2015). The prototype, shown in image (7), was capable of reeling, but not managing, its tether. The motivation for the TReX design is meant to address a common limitation of all prior systems, which is a lack of advanced mobility on steep terrain; no prior system has demonstrated the capability of turning significantly outside the direction of applied tension to drive laterally with respect to the slope. This disadvantage risks tether entanglement when navigating around obstacles, and limits the robot to drive in a straight line away from its anchor, hindering mapping efficiency.

2.2 | Three-dimensional mapping

We are motivated by the idea of lidar-based geologic mapping because it is more efficient than manual survey and also provides a means to investigate rock structure and composition using lidar intensity returns (Osinski et al., 2010). Since we are interested in producing a map from a rotating lidar mounted to a moving vehicle, we can formulate our problem as a simultaneous localization and mapping (SLAM) problem (Smith, Self, & Cheeseman, 1990). The landmark-based SLAM approach is commonly used to solve this problem, where the state of the robot (i.e., the trajectory and map) is estimated given lidar measurements (i.e., range/bearing to 3D points; Cole & Newman, 2006; Durrant-Whyte & Bailey, 2006). Given that our robot is always in motion while scanning, we require a tool to recover its trajectory in 3D space. Bosse and Zlot (2009) use offline, batch scan matching to find a transform between two scans that can be used to approximate the sensor's trajectory in 3D space without the need for additional odometric measurements. Zhang and Singh (2014) expand on this with a continuous-time lidar odometery and mapping (LOAM) approach that uses high-rate, low-resolution lidar odometry to provide a motion estimate to use in low-rate, fine-resolution scan registration. Without modification, LOAM would not work for TReX because (a) scanning is coupled to the robot's motion (i.e., lidar odometery fails while stopped), and (b) its environment is highly unstructured (i.e., lacks planar surfaces and edges). One solution is VLOAM, also from Zhang and Singh (2015), which integrates additional measurements from VO to estimate the robot's motion during a scan.

As mentioned previously, we test two methods to estimate the robot's trajectory and produce a global map from lidar measurements. The first is a lidar-only, continuous-time approach from Anderson and Barfoot (2015), which uses a constant-velocity motion prior for the robot during scan collection and allows for any-time trajectory sampling. As asynchronous lidar measurements arrive, they are associated to a queried transform that can be used to rectify individual 3D scans before alignment into the global map. The critical difference between this approach and LOAM, is its use of a physically motivated motion prior, which enables it to work for TReX. Once a scan has been rectified, it is aligned into the global map using an efficient form of the ICP algorithm (Pomerleau, Colas, Siegwart, & Magnenat, 2013). The second method also relies on ICP for scan matching and is similar to VLOAM, in that it leverages VO as a motion before minimize scan distortion (Kubelka et al., 2015). While the continuous-time method requires the minimum number of sensors (i.e., lidar only), the VO-aided approach is better equipped to capture the robot's complex motion in highly unstructured environments for mapping.

3 | SYSTEM DESIGN OF TReX

The operational concept for the TReX system is shown in Figure 3. McGarey et al. (2015) first introduced TReX as a system that can

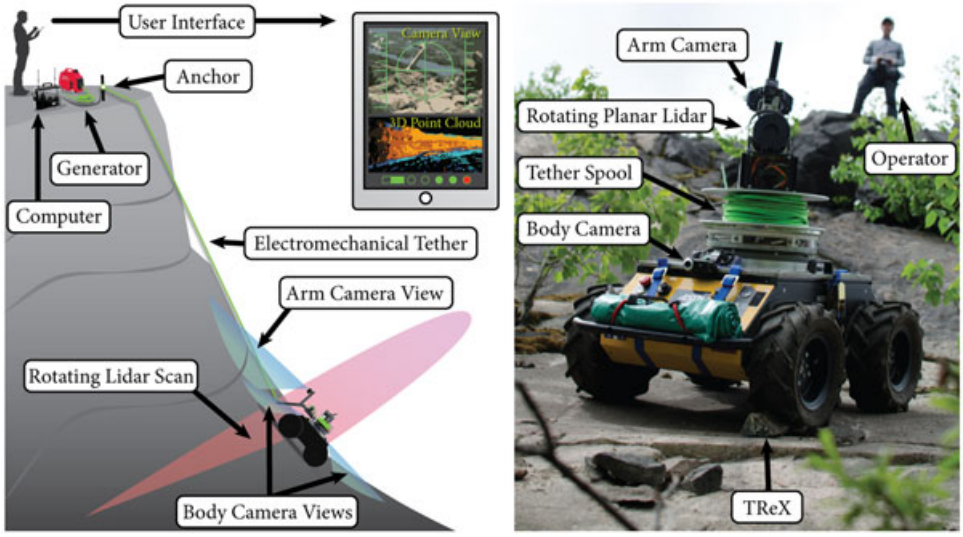

FIGURE 3 Tethered Robotic eXplorer: The illustration on the left is an operational concept for a typical TReX geologic surveying mission. TReX is anchored and deployed near the cliff's edge to map the steep terrain using an on-board lidar. The right image shows an actual mapping field deployment [Color figure can be viewed at wileyonlinelibrary.com]

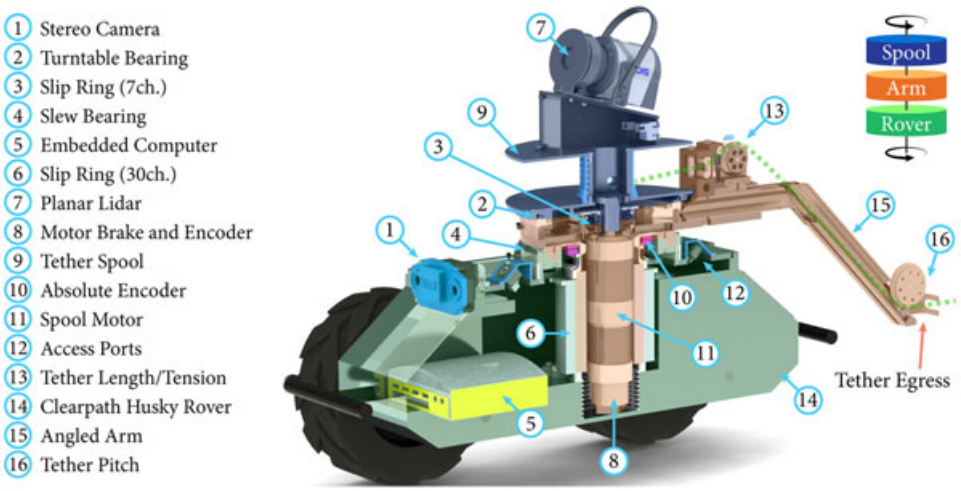

FIGURE 4 TReX cut view: The rotating elements of TReX are highlighted by color. The tether arm (orange) rotates passively in the direction of applied tension. The spool (blue) is actuated with respect to the tether arm. The rover (green) can rotate in place on steep slopes to drive laterally on the steep terrain [Color figure can be viewed at wileyonlinelibrary.com]

both rotate in place regardless of the direction of applied tension due to a passively rotating tether arm, and generate 3D scans of the environment through tether spool rotation. The advanced mobility of the platform allows for turning in place and driving laterally on steep terrain provided sufficient wheel traction.

3.1 | Continuous rotation

To navigate laterally on steep slopes, the TReX design allows for continuous rotation while under tension; a tether management payload attaches to a conventional, wheeled rover and passively rotates about its center (yaw) axis. The payload is mounted to a Clearpath Husky A200 rover, which is a four-wheeled, skid-steered robot base. The tether, which terminates at the rotational center of the robot and tether management payload, is deployed through a tether arm that passively rotates in the direction of applied tension. The tether arm is also angled at the tether's egress point, which has the effect of providing stability on steep terrain by aligning[1] the tensional force with a virtual line passing through the vehicle's center-of-mass. The tether is reeled in and out using a motorized spool, which is not coupled in any way to rover rotation. To visualize the complex rotational freedom of the TReX design, Figure 4 provides an annotated cut view with color-coded, rotating elements highlighted. To accomplish the rotation, we have mounted the tether management payload on a slew bearing. Power and data are transmitted between the

[1]The tether arm length can be adjusted, that is, "trimmed," for better alignment.

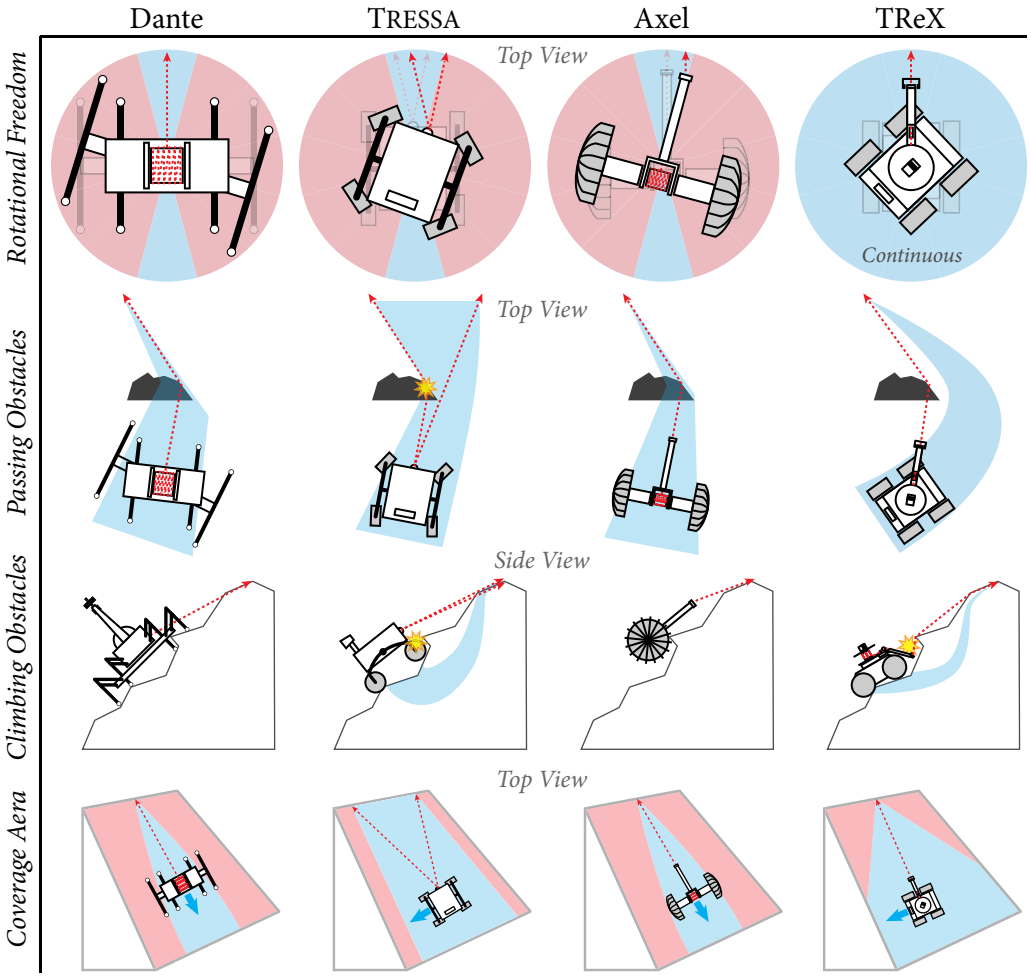

FIGURE 5 Mobility Comparison to Other Systems: The mobility of Dante, TRESSA, Axel, and TReX are qualitatively compared in the illustrations above. We note that these illustrations are not informed by prior research, and instead, are created by looking at the design of past systems to make a cartoon mobility comparison. Rows represent mobility metrics and columns correspond to tethered systems. All vehicles (except TRESSA) manage tether on board. Tethers are dashed red lines and tether-to-obstacle contacts are yellow stars. The light blue and red shaded regions represent feasible and infeasible rotations/paths, respectively. Blue arrows indicate vehicle heading. Overall, the TReX design enables continuous rotation under tension on steep terrain, which improves obstacle navigation, increases coverage area, and makes mapping more efficient [Color figure can be viewed at wileyonlinelibrary.com]

rover base and payload using a multichannel slip ring with a hollow center. The spool motor is conveniently suspended within the hollow center of the slip ring and is fixed only to the base of the tether arm. Power is transmitted through the slip ring and into the motor to rotate a shaft that is coupled to the tether spool. The spool rotates on a separate turntable bearing and is electrically linked to the tether arm by a second, hollow-center slip ring, which allows the motor shaft to pass through. An electronics compartment at the top of the spool distributes power to the top-mounted lidar (light detection and ranging sensor), and is the connection point for the tether. The tether passes AC power and Ethernet data into the electronics compartment. AC is converted to DC on board, which is used to charge a battery, while the Ethernet is linked to an embedded computer located in the rover base. The end result is that TReX can rotate continuously on steep terrain, provided sufficient wheel traction, while the tether spool rotates to manage tension and generate 3D scans.

3.2 | Comparison to other systems

Below, Figure 5 compares the mobility of TReX with past systems. TReX's ability to rotate continuously under tension on steep terrain is beneficial for obstacle navigation and efficient mapping. Each platform is evaluated by the following metrics.

1. *Rotational freedom*: Prior systems do not rotate significantly outside the direction of applied tension. TReX has a passively rotating tether arm that allows rotational freedom on steep terrain, provided sufficient wheel traction.
2. *Passing obstacles*: Tether-to-obstacle contacts create intermediate anchors, which must be removed in order for the robot to return safely. TReX has the ability to rotate and drive laterally around an obstacle instead of surmounting it.
3. *Climbing obstacles*: Despite the advanced rotational ability of TReX, there are still challenges to navigating extreme terrain. While

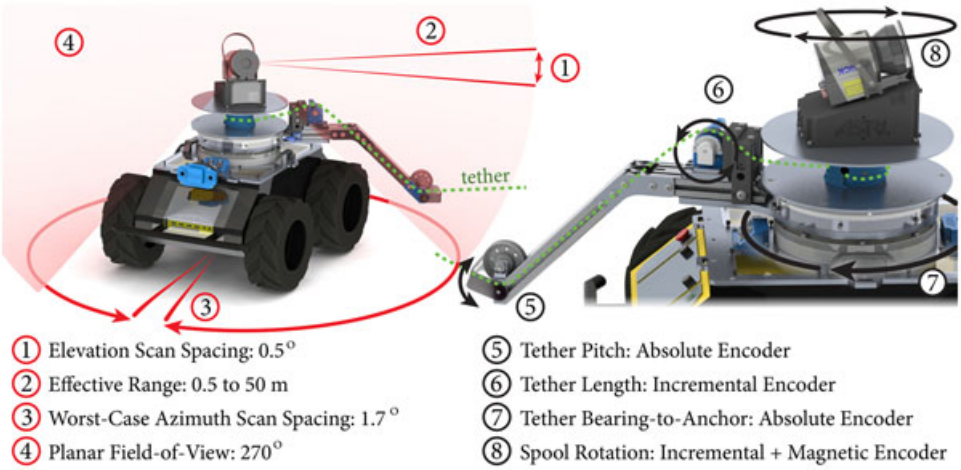

FIGURE 6 TReX sensor configuration: The left image provides 3D mapping specifications for the lidar, while the right indicates the tether and payload orientation sensor arrangement [Color figure can be viewed at wileyonlinelibrary.com]

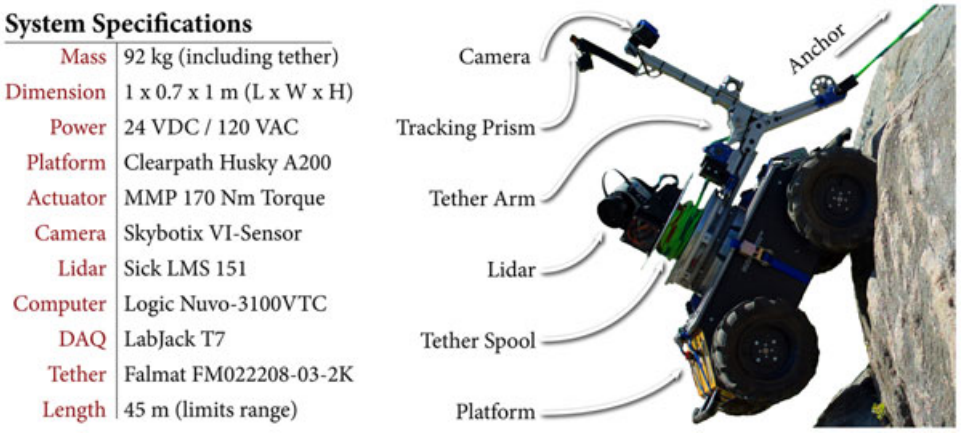

FIGURE 7 Specifications: Fielded TReX system. We note that a stereocamera is mounted on a mast, which attaches to the rotating tether arm. This configuration allows for passive stabilization of the camera's field-of-view pointing in the direction of the taut tether [Color figure can be viewed at wileyonlinelibrary.com]

Dante and Axel are tailored for navigating over large obstacles, TReX's size and limited ground clearance can cause the robot to get stuck if no alternative path exists around a difficult obstacle.

4. *Coverage area*: The ability to drive laterally on steep terrain allows TReX to sweep back and forth to cover more area in a single traverse. Other systems are limited to travel mostly linear paths, which means that the anchor must be relocated to cover and map new areas.

3.3 | Sensor configuration

The sensor configuration of the TReX platform is illustrated in Figure 6. TReX has the ability to make a complete 3D scan of the environment through the rotation of an attached 2D lidar. Due to the single-actuator design of the tether management payload, 3D scanning is dependent on the deployment of tether through vehicle motion. During lidar rotation, the worst-case, azimuth scan spacing[2] is 1.7°, which is a function of the maximum spool rate (0.23 revolutions/s) and the lidar's scan frequency (50 Hz). The upward-facing orientation of the lidar allows for scanning enclosed environments, like caves and crevices, but also works for planar surfaces, like cliffs and dam walls. Figure 6 also illustrates how measurements of the payload's orientation and attached tether are made. To create accurate maps of the environment, we need to know the orientation of the rotating lidar with respect to the robot base at all times. To accomplish this, we use a series of encoders to measure (a) the angle of the tether arm with respect to the robot base, and (b) the angle of the spool with respect to the tether arm. We also use (a) as a tether bearing-to-anchor measurement in conjunction with an encoder that measures tether length to aid in localizing obstacle-to-tether contacts. Tether pitch is measured at the egress of the tether arm, and offers a basic measurement for tether tension. To accurately measure tension for

[2]In spherical coordinates, the worst-case azimuth scan spacing is the angle between a pair of points observed between two consecutive scans at the same elevation or polar angle.

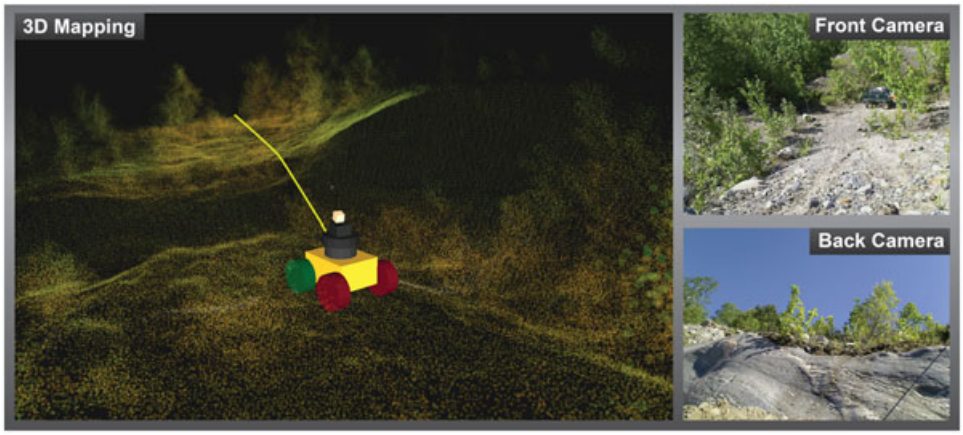

FIGURE 8 User Interface: A remote user monitors and teleoperates the robot by viewing the live map and cameras, which are transmitted over tether. The tether has been illustrated for reference [Color figure can be viewed at wileyonlinelibrary.com]

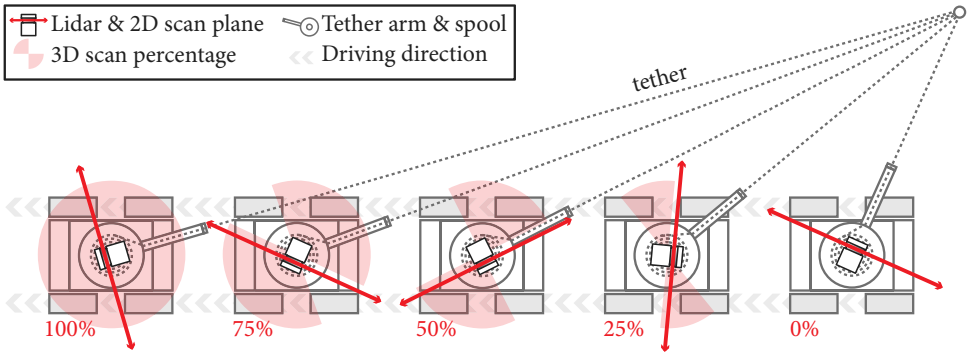

FIGURE 9 Generating a 3D scan: As illustrated, a 3D scan is built from a series of 2D scans only when the robot drives and deploys its tether, which causes 3D scans to be motion distorted. Generally, the robot will need to travel 0.5 m to generate a single scan [Color figure can be viewed at wileyonlinelibrary.com]

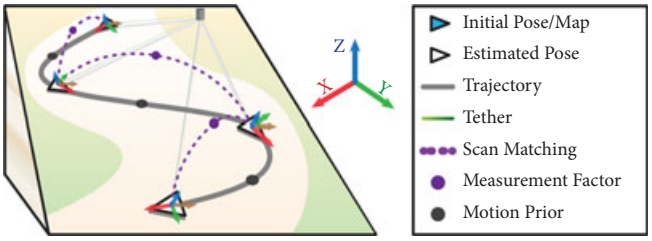

FIGURE 10 Building a map: This pose graph represents the scan matching process used to create a global map. Triangles represent the state (i.e., pose and map) being estimated. Before matching, the trajectory of the robot is estimated with either a constant-velocity or VO-aided motion prior. Scans can be matched into the global map either sequentially or in a batch, sliding-window setup [Color figure can be viewed at wileyonlinelibrary.com]

the purpose of automatic tension control, we use a piezoelectric sensor integrated into a pulley mechanism that also measures tether length.

3.4 | Fielded system

Figure 7 shows specifications for the fielded TReX system. To assist with remote piloting in the field, the user interface shown in Figure 8 was developed to allow real-time monitoring of multiple cameras on the robot while observing the construction of a point-cloud map.

4 | MAPPING METHODOLOGY

Figure 9 illustrates how a planar lidar fixed to the robot's tether spool is used to generate a 3D scan as TReX drives. The slow rotation of the lidar while in motion results in scan distortion analogous to the rolling-shutter effect in passive cameras. To complete a single 3D scan, the spool must rotate by 180°, which translates to 0.5 m of distortion along the direction of travel at full speed. For comparison, a car with a Velodyne lidar, scanning at 10 Hz, would only need to travel at 5 m/s (18 km/hr) to produce 0.5 m of distortion. However, in our case, the rotational speed of the lidar will not always be constant due to a coupling of spool rotation with vehicle motion, which leads to distortion that is not uniform in time.

Any distorted scan can be rectified by estimating the trajectory of the lidar or robot during collection. Given the rough terrain and slow speed of the robot, wheel odometry cannot be relied on. Alternatively, one approach is to assume a constant-velocity model for the robot during the collection of a single scan to handle

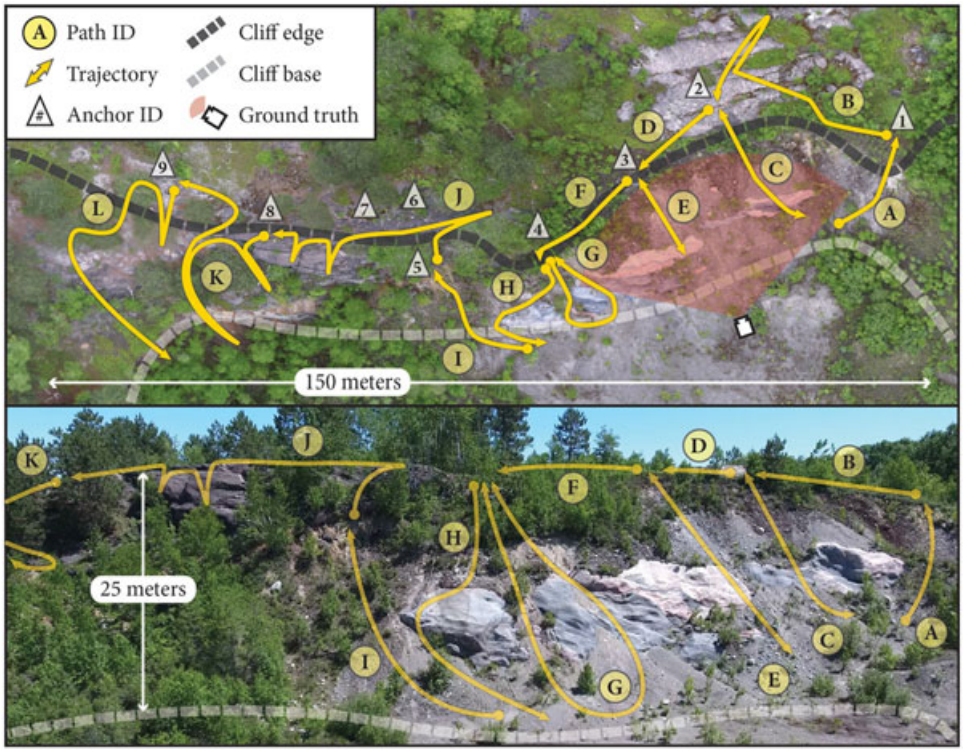

FIGURE 11 Experiment site: The paths driven during the experiment are illustrated on aerial images. The area marked as "ground truth" was mapped by a stationary Leica Total Station. Being that the cliff is covered with vegetation, we use TReX to navigate below the tree canopy for in situ mapping [Color figure can be viewed at wileyonlinelibrary.com]

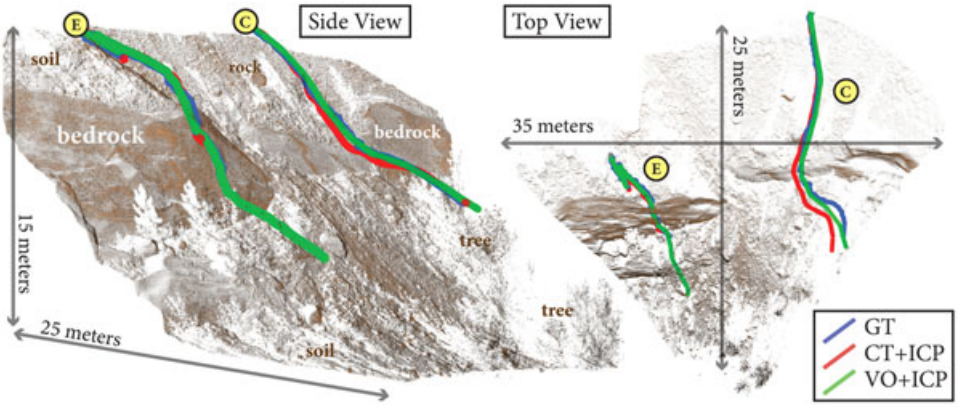

FIGURE 12 Trajectory comparison: Two intensity-colored, ground-truth point clouds are shown. The "side view" shows the slope, which ranges from 30° to 60° inclination. The outgoing position of the robot was recorded to provide ground truth (GT) while driving on Paths C and E only. The VO-aided ICP estimate, VO + ICP, outperforms the continuous-time approach, CT + ICP. We note that GT and CT + ICP are not complete for Path E, which is due to target loss and estimation failure resulting from the robot's complex motion [Color figure can be viewed at wileyonlinelibrary.com]

asynchronous measurements from the lidar. The continuous-time approach uses Gaussian-Process (GP) regression to allow for any-time trajectory querying using GP interpolation, which means that the sensor's pose can be queried at measurement time. The benefit of this approach in SLAM is that it only relies on lidar data and uses a physically motivated motion prior (i.e., white noise on acceleration). For more on this continuous-time approach, including detail on pose-graph architecture and the constant-velocity model and implementation, see Anderson and Barfoot (2015). Additionally, Tang, Yoon, Pomerleau, and Barfoot (2018) provide more details about the lidar-based, continuous-time approach specific to bias estimation for a lidar motion estimation. In extreme cases, when the constant-velocity model fails to capture the true motion of the robot, the continuous-time approach will not work (see Figure 19). Accordingly, we test a second method to handle distortion that uses VO as a motion prior for the robot's trajectory during a single scan; VO is generally accurate over short distances and is better suited to capture complex robot movements, provided that the

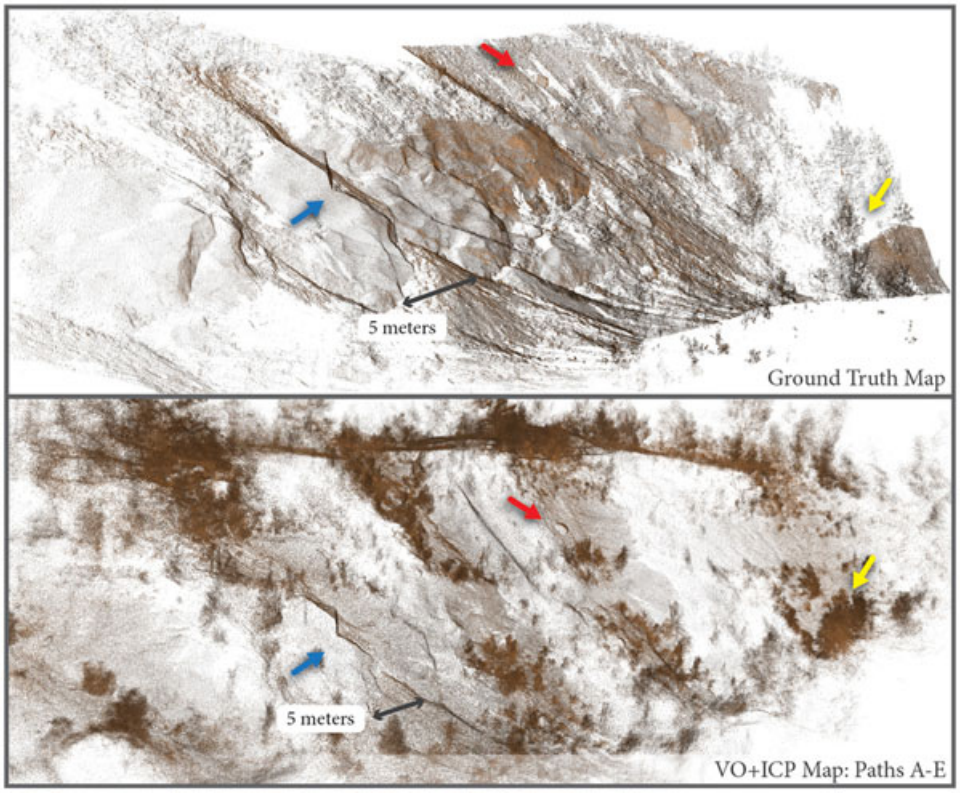

FIGURE 13 Global map comparison: Global point clouds of the unobstructed terrain are compared. The ground-truth map shows the terrain visible to the LTS from a remote position. The VO + ICP map, which encompasses more area than the ground-truth scan, combines estimated point clouds from Paths A–E, which were aligned manually. Common features are indicated by color-coded arrows [Color figure can be viewed at wileyonlinelibrary.com]

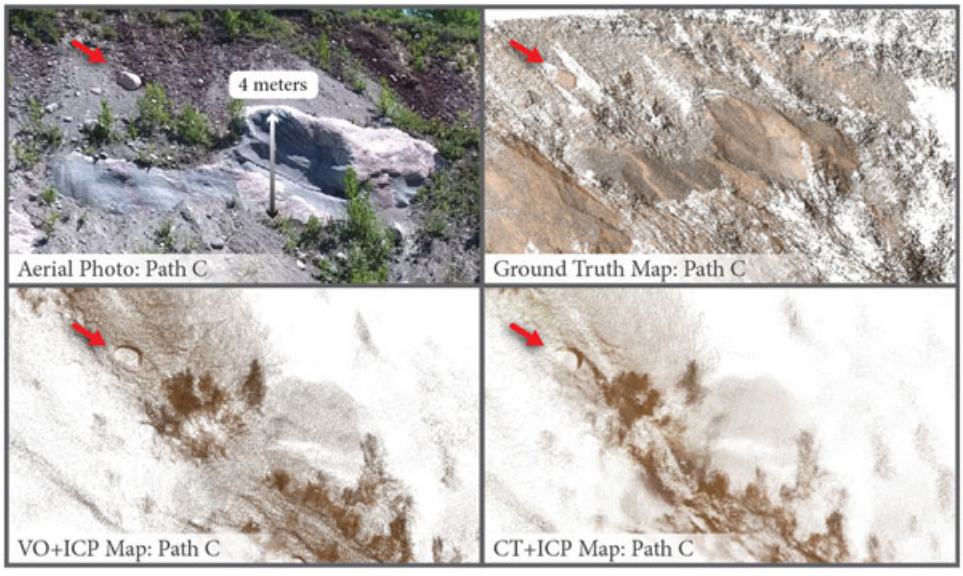

FIGURE 14 Local map comparison: An aerial photo is compared with close-up, virtual images from ground-truth, VO + ICP, and CT + ICP maps colored by point intensity. The rock shown by red arrows in Figure 13 is marked here as well. While the ground truth is most dense and clearly shows rock features, VO + ICP is our best estimate and is noticeably more detailed than CT + ICP. The estimated maps are sparse due to limited observation time in the target area (e.g., not enough scans were generated). This is also a case where CT + ICP works for a segment of the full trajectory. Generally, the robot's motion is too complex for CT + ICP to work on more challenging trajectories [Color figure can be viewed at wileyonlinelibrary.com]

field-of-view and lighting conditions are stable. We use an existing VO package[3] to output pose estimates during scan generation at the frame rate of the camera (10 Hz), and rely on a linear-time interpolation function in ROS to associate incoming lidar data to pose estimates. Once scans are rectified, we perform ICP matching[4] to align new scans into a global map. Figure 10 illustrates the mapping problem.

The mapping pipeline involves tunable parameters. The continuous-time approach requires providing an expected velocity variance for translation and rotation, in addition to a sliding window size over which to optimize. Accordingly, we assume that most of the movement occurs in x, the driving direction of the vehicle, bounded at 1 m/s with minimal variance in y and z translation (0.1 m/s) and rotation (0.001 rad/s). The window size is set to optimize over the last six scans collected, which allows for a fast solve without sacrificing mapping accuracy. The ICP pipeline involves tunning a point-to-point expected standard deviation parameter, which we set to 0.01 m, and a random sampling parameter to reduce the density of the incoming point cloud, which is set to down sample points by 70% in order perform fast matching to the global map.

5 | FIELD DEPLOYMENT AND MAPPING RESULTS

5.1 | Field deployment

Mapping experiments were performed in an outdoor, open-pit mine located in Northern Ontario, Canada. This location features a steep cliff, where bedrock is exposed but is hidden by vegetation. Figure 11 provides aerial images of the site that have been annotated with the paths taken to map the terrain. TReX was teleoperated for the experiment due to the extreme conditions. Note that much of the cliff is covered by vegetation, meaning that remote survey alone cannot be used to map the contiguous rock outcrop.

5.2 | Mapping results

While driving on Paths C and E, the 3D position of a marker fixed to the robot was recorded by a Leica Total Station[5], which has a prism-tracking and point-scanning accuracy of 1 and 2 mm, respectively. Figure 12 illustrates the ground-truth trajectory overlaid on a dense, ground-truth point cloud. For comparison, we show trajectory estimates from our continuous-time (CT) and VO-aided ICP pipelines. We note that the full trajectory is not shown because it extends off the visible point cloud. Instead, we plot a portion of the outbound trajectory for clarity. As shown, the VO-aided estimate is closest to ground truth, which is true for all runs. In fact, the CT approach only works when the robot's true motion is smooth and the environment is sparsely vegetated, as later discussed in Section 6. On a large scale, the combined VO-aided map (Paths A–E) is comparable to ground truth, and actually covers more area as shown in Figure 13. Looking closer, Figure 14 compares a portion of the map produced from Path C. Although the VO-aided map is clearer than CT, both fail to capture the rock outcrop better than ground truth because (a) individual scans collected by TReX are relatively sparse, and (b) an insufficient number of scans were collected of the target area. Lastly, Figure 15 provides a map collected by TReX from a densely vegetated, cluttered environment, where the robot navigates below the tree

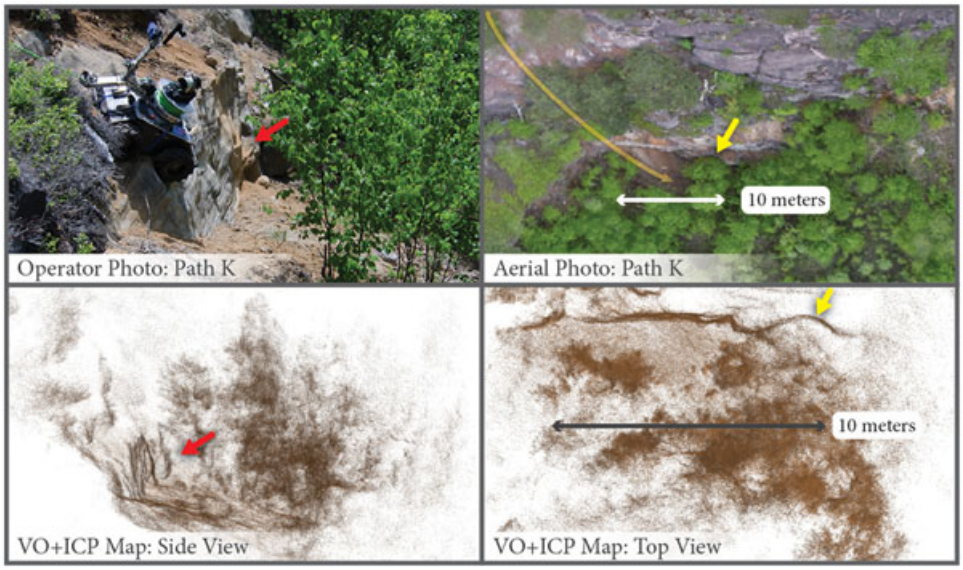

FIGURE 15 Mapping cluttered environments: This example highlights the benefit of the TReX platform, which can navigate in cluttered environments to explore terrain occluded from remote view. The photos show a heavily vegetated, hard-to-reach area on Path K where bedrock is exposed. Virtual images from the VO + ICP estimated point cloud are compared images. Arrows indicate shared features between the image and map. A portion of Path K is also superimposed on the aerial photo [Color figure can be viewed at wileyonlinelibrary.com]

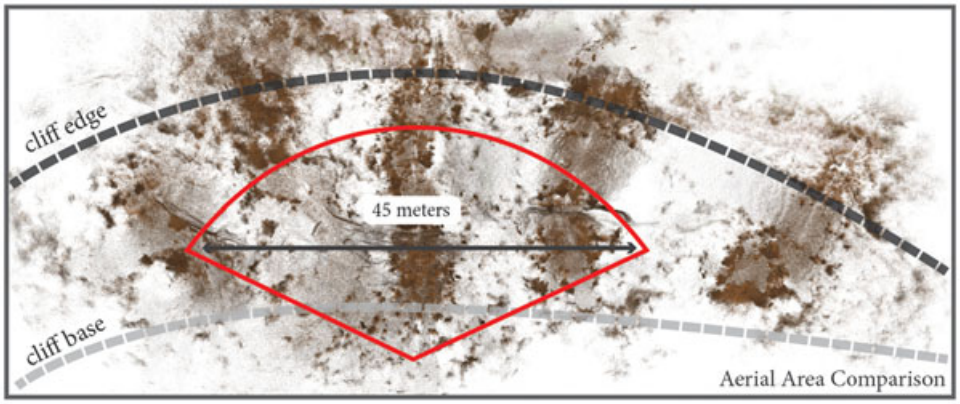

FIGURE 16 Coverage-area comparison: This top-down aerial view compares the area mapped by ground truth (highlighted in red) to area mapped by TReX. The map comes from a combination of point clouds produced on Paths A–E using the VO + ICP approach (Paths I–L are not pictured). The main point is that TReX can access and map areas that are not visible remotely (e.g., the top of the cliff or below the tree canopy) [Color figure can be viewed at wileyonlinelibrary.com]

canopy and surveys a rock feature that is not visible remotely (Figure 16).

6 | LESSONS LEARNED

6.1 | Systems design

1. *Mobility*: Figure 17 provides a collection of images that both highlight the robot's advanced mobility on steep terrain, and demonstrate limitations of the platform. In general, TReX was successful in navigating very steep slopes, regardless of the terrain type (e.g., rock, sand, or grass). With the exception of the inverted slope in Figure 17.4, the angled tether arm aligns tensional force with the robot's center-of-mass, keeping all tires in contact with the surface. Figure 17.5,6 shows examples of TReX driving laterally under tension, which made it possible to visit and map more terrain during a single traverse. Despite the success of the deployment, there were several failures, which underline key limitations of the platform. In Figure 17.7, TReX is shown after tipping over, which occurred while driving parallel to the tether on a steep, angled surface. The fall indicates that (a) the center-of-mass is too high, and (b) the robot would benefit from some form of passive differential suspension (e.g., rocker-bogie system) to accommodate for uneven terrain. Several considerations should be made related to mobility; (a) the mass distribution of the robot should be close to the ground to prevent tipping, and (b) turning-in-place with a skid-steered tethered robot is a high-torque action that requires sufficient motor power. While TReX is a successful example of a conventional, ground robot outfitted to access extreme terrain, the base platform is underpowered (considering the terrain) and not ideal for traversing steep, rocky environments. Instead, the design should consider a differential suspension (e.g., rocker-bogie system) for navigation on uneven terrain, more powerful drive motors, and a reduction in size for increased stability.
2. *Size*: The current size and mass of TReX (1 m^3 and 100 kg) are limiting factors to its adaptation and usefulness in the field. Currently, at least two operators are required for deployment. When considering scale, both the robot and base station (computer, anchor equipment, and generator) should be sized such that they can be stored in a large backpack and carried by a single operator. The size reduction would also allow for a thinner tether to be used, which, depending on the spool capacity, would increase the operational range of the robot.
3. *Tension measurement*: The TReX design measures tension using a force-plate assembly on the tether arm, where small fluctuations in the sensor's structure are converted to a calibrated voltage output. The drawback of this approach is that the rigid configuration allows for minimal shock absorption or flex, which makes the output of the sensor noisy (especially at low tensions). Currently, shock is absorbed directly into the tether arm, which is not ideal for structural safety, as the strength of metal components will degrade with continued use. An alternative approach would be to account for shock absorption using a spring-mass damper system, which could ensure consistent sensor readings and better tether control.
4. *Tether damage*: Tether can be damaged in two ways, (a) by the environment, or (b) by the tether management system. Handling (a) is less straightforward and would require anchor planning, which is beyond the scope of this study. Handling (b) is accomplished by limiting tight bends, twisting, and abrasion within the system. Our tether management system uses a set of pulleys to passively guide the tether on/off the spool as the robot

[3]Fast Odometry from Vision Huang et al. (2011), package available: https://github.com/srv/fovis.

[4]Libpointmatcher Pomerleau et al. (2013), package available: https://github.com/ethz-asl/libpointmatcher.

[5]Model: Leica Nova MS50 MultiStation

FIGURE 17 Platform evaluation: TReX's advanced mobility on steep terrain is demonstrated through visual examples during the field deployment. Images 1–3 show TReX successfully navigating steep rock faces. Image 4 shows how the robot's front tires can lift off the rock due to excessive slope and high tension on the tether. Images 5 and 6 show the lateral mobility of the robot while under tension. Image 7 shows TReX just after tipping over, which was caused by platform instability when navigating tangent to an angled surface. Image 8 illustrates a common limitation of using a tether; when the taut tether contacts rock, abrasion or severe bending can result in damage [Color figure can be viewed at wileyonlinelibrary.com]

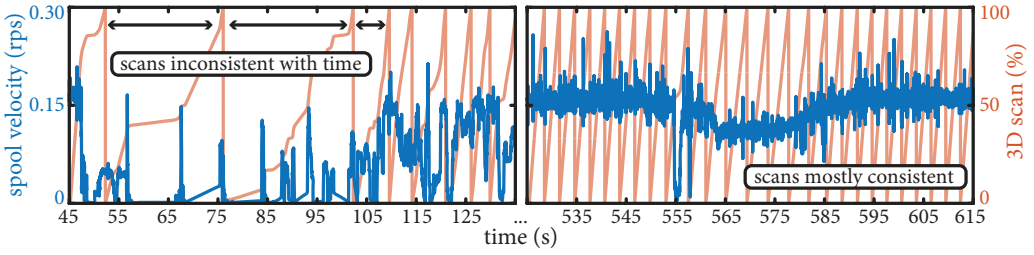

FIGURE 18 Scan completion over time: The correlation of spool velocity, measured in half rotations-per-second (rps), to percentage scan completion is shown at select time intervals. We note that a full scan only requires a half rotation of the spool. The important take away is that scan completion varies with time, which violates the constant-velocity assumption of the CT method [Color figure can be viewed at wileyonlinelibrary.com]

moves. In some instances, the recommended bend radius for the tether is exceeded due to the size of the pulley, which results in degradation of the internal wires over time. This degradation is made worse by tether twist, which is caused by continued spooling. We also do not incorporate a level-wind system to prevent non-uniform tether buildup on the spool, which in some cases results in tether "knifing" (i.e., the outer layer of tether slips between the inner layer and becomes caught) Figure 17.

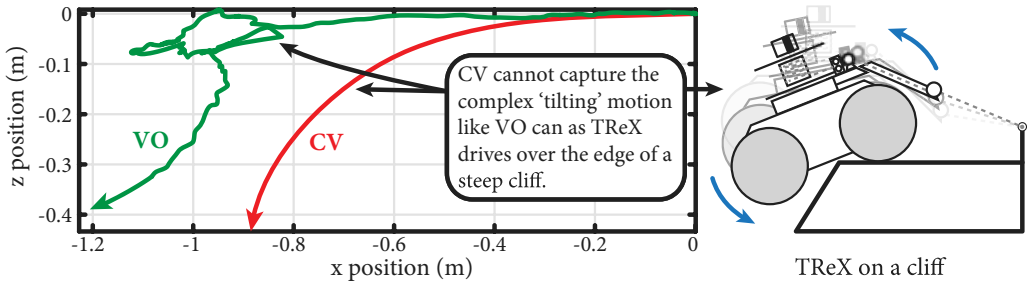

FIGURE 19 Motion prior comparison: We show the robot's estimated motion for a small portion of the trajectory from the start of a path until just after first descent. The trajectories are plotted as a vertical profile (*x*–*z* plane). The constant-velocity motion prior, CV, forces a smooth, arcing trajectory estimate, which fails to capture the complex tilting motion accurately captured by VO. The "loop" in VO occurs after the robot rocks back and forth in place just after driving over edge [Color figure can be viewed at wileyonlinelibrary.com]

6.2 | Environment mapping

1. *Mapping challenges*: Given the mapping performance discussed in Section 5.2, we consider the factors that cause the continuous-time (CT) approach to perform worse than the VO-aided approach in complex, unstructured environments. One reason is illustrated in Figure 18, which shows the correlation of spool velocity to 3D scan completion over time. For two sample intervals, we see that the time to complete a scan varies strongly, which implies that TReX, whose spool velocity is coupled to vehicle motion, may violate the constant-velocity model used in CT estimation. One way to deal with this problem is to add additional keyframes (i.e., pose estimates along the trajectory), which would make the velocity assumption arbitrarily better, but also have the effect of slowing down the pipeline. Currently, keyframes are dropped at the completion of each scan (e.g., the robot drives ~0.5 m), which allows for running the pipeline in real time. Instead of inserting more keyframes, we set the velocity before zero between segments of the trajectory where gaps in measurement time occur. However, we must contend with a greater issue, which is that the velocity prior fails to truly capture the complex motion of the robot driving on extreme terrain. Figure 19 best illustrates this problem; the zoomed-in view shows the estimated trajectory from VO compared to the constant-velocity estimate from CT just as the robot drives over the edge of a cliff. Assuming constant velocity, the robot's motion is estimated to be a smooth arc, when in reality, the robot tilts or rocks at the edge of the cliff before descending. Conversely, VO is able to capture this complex motion. However, VO can fail if the environment is overly cluttered and lighting is too dynamic, which occurs when navigating through dense vegetation (i.e., strong shadows and obstructed vision from hanging leaves). Another challenge for mapping in the field is that it is difficult to generate dense, minimally distorted point clouds given the operational environment. Figure 20 illustrates this idea by showing how cluttered environments impact scan density and quality; throughout a single traverse, the quantity and average depth of 3D points vary as the robot passes through vegetation. The low average depth indicates that most points lie within 3 m, making it harder to scan distant targets. In terms of point quantity, even the most dense scans are still sparse, with most of the scan being lost to the sky. For comparison, a Velodyne lidar can generate between 100 and 200 *k* points per scan, which is an order of magnitude more than TReX. Therefore, it would be beneficial to use a 3D scanning lidar to produce high-quality, detailed maps.
2. *Lidar configuration*: The lidar should rotate independently of vehicle movement to enable targeted, dense mapping. Due to its increased availability and reduced form factor, 3D lidars would be beneficial for mapping because they limit scan distortion. Another concern is that falling rocks or debris can strike and damage the

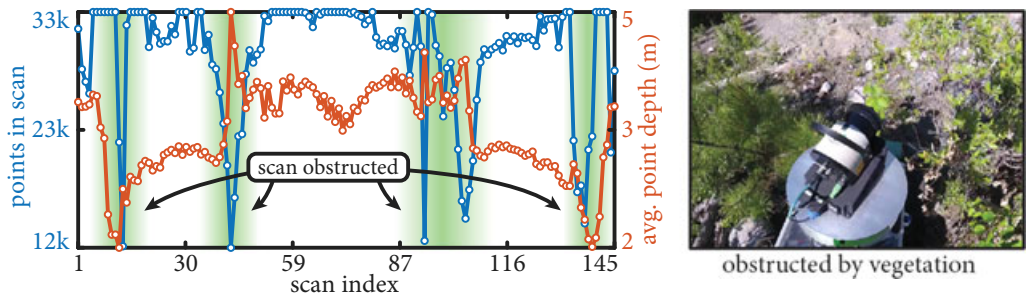

FIGURE 20 Scan quality: The quantity and average depth of 3D points are shown per scan collected on a typical trajectory. The shaded regions represent degenerate scanning conditions that result from navigating through vegetation as shown in the example image. The result is that each 3D scan is generally sparse and shallow in depth, which decreases the likelihood of accurate scan matching [Color figure can be viewed at wileyonlinelibrary.com]

sensor if not shielded. Accordingly, the lidar should be mounted so that rocks falling from above cannot hit the sensor's lens or sensitive electronics.

3. *Intensity mapping*: Given our interest in leveraging intensity returns from the on-board lidar to infer characteristics about the environment, the problem of in situ mapping, where the most intense returns come from nearby points, must be addressed through range correction of the lidar. Currently, we assume a factory-calibrated range correction, which makes it difficult to detect intensity differences in rocks or nearby features from scans collected by TReX.
4. *Sensors for mapping*: Robustly estimating the trajectory of the robot for mapping would benefit from additional sensors beyond a camera, lidar, and wheel odometry. From experience, there are degenerate conditions that cause the camera and lidar to fail (e.g., navigating through very dense vegetation), which could be aided by incorporating inertial and tether measurements. Inertial measurements would be useful for tethered robots because they operate on steep, inclined terrain, which means that an IMU or inclinometer can be used to extract global information about the robot's orientation with respect to gravity. Also, tether length is useful for constraining the robot's translational distance away from a known starting point.

7 | CONCLUSION

We have evaluated how tethered mobile robots can be used to effectively explore and map extreme environments for geologic survey and structural inspection. When a mobile robot is outfitted with a supportive electromechanical tether, it benefits from continuous power and hard-wired communication to a remote base station. This field report details the development and field deployment of the Tethered Robotic eXplorer (TReX) to map extremely steep, cluttered terrain. We show, through a review of prior systems, that TReX enables enhanced mobility using a center-pivoting, tether-management system. We deploy TReX in the field to demonstrate its mobility as well as to evaluate mapping functionality. Mapping with TReX is a challenge because scanning is coupled to the robot's motion and tether reeling. To generate accurate 3D maps of the environment from motion-distorted scans, we evaluate (a) a continuous-time approach that relies on a velocity-based motion prior, and (b) a VO-aided approach that leverages odometry from a stereocamera. Both methods are used to compute a trajectory estimate, which can be used to rectify distorted scans before ICP alignment into the global map. Each pipeline was evaluated with data collected during the field trial. Our results indicate that the VO-aided approach outperforms the continuous-time method because it best captures the robot's complex motion in dynamic, unstructured environments. Moreover, we test a customized tethered robot in a relevant field experiment and provide lessons learned from design through deployment.

Looking forward for tethered robots, it will be important to integrate new autonomy to allow for unsupervised exploration of extreme environments. Consider the example scenario shown in Figure 21, where an operator hikes to an interesting area, sets up the base station, and deploys the robot to explore and map. To do this operation autonomously, the robot will start by using on-board sensors to plan a safe, tangle-free path down the terrain, where Teshnizi and Shell (2014) have proposed tethered, path-planning algorithms in prior work. However, to extend path-planning theory to work for real, tethered robots, we would first need to determine where the obstacles are and how the tether interacts with them. The first step could use aerial images to generate a coarse, a priori map, from which obstacles are determined Abad-Manterola (2012). Once on site, the robot can generate a dense scan of the environment, match that to the coarse map, and plan a descent path that covers as much of the terrain as possible. Next, the robot can either repeat back along the same path to unwind from added anchors McGarey,

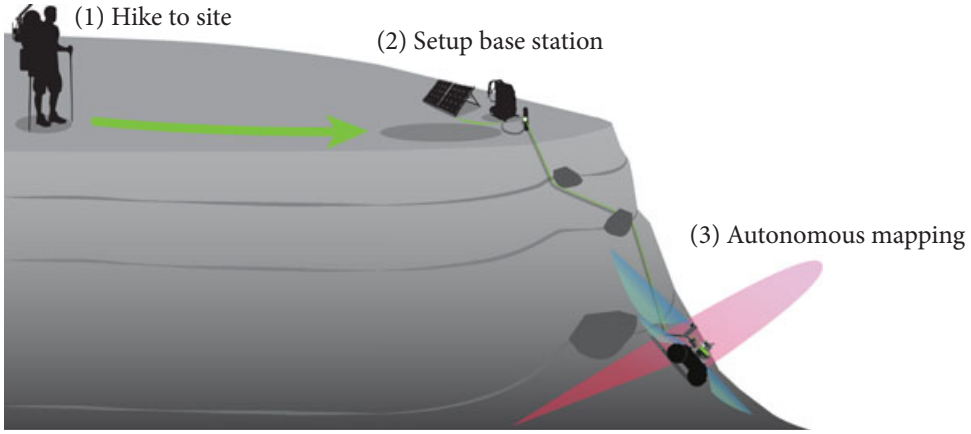

FIGURE 21 Future concept: We illustrate a future concept for the autonomous mapping of cliffs with a tethered robot. In this scenario, the operator hikes to an interesting site, assembles the base station, and deploys a tethered robot, which can plan paths down the slope to expand the mapping frontier and return safely along a previously driven path [Color figure can be viewed at wileyonlinelibrary.com]

Polzin, and Barfoot (2017) or continue to explore safe paths that expand the frontier of the estimated map. It would also be beneficial to integrate autonomous path following with anchor detection, where McGarey, MacTavish, Pomerleau, and Barfoot (2017) details a novel SLAM technique for anchors, which could potentially allow for extending Visual Teach & Repeat (VT&R) to work within safe, boundary regions defined by detected anchors. Most importantly, the operator can monitor mapping progress and relax while the robot autonomously explores all the accessible terrain from a given anchor location. To map more terrain, the operator can move the initial anchor and deploy the robot again. By leveraging off-board power, the robot can repeat this task until the user is satisfied that the targeted area has been mapped. Looking further ahead, the autonomous exploration of cliffs and caves on other planets will require additional consideration for how the robot is transported to, and anchored from, the cliff. Matthews and Nesnas (2012) show that an attached, companion robot can be used as an anchor, power supply, and communication intermediary for data transmission. This approach has the benefit that the "anchor" can be moved. Alternatively, a targeted, stationary lander with an attached tethered robot could be sent to the edge of a cliff. Unfortunately, this approach leaves little margin for landing error and would only allow for a single site to be explored.

ORCID

Patrick McGarey http://orcid.org/0000-0003-0188-5114

REFERENCES

Abad-Manterola, P. (2012). Axel rover tethered dynamics and motion planning on extreme planetary terrain. (PhD thesis). California Institute of Technology.

Anderson, S., & Barfoot, T. D. (2015). Full STEAM ahead: Exactly sparse gaussian process regression for batch continuous-time trajectory estimation on se (3). In: *2015 IEEE/RSJ International Conference on Intelligent Robots and Systems (IROS)* (pp. 157–164)

Bares, J. E., & Wettergreen, D. S. (1999). Dante II: Technical description, results, and lessons learned. *The International Journal of Robotics Research*, *18*(7), 621–649.

Bosse, M., & Zlot, R. (2009). Continuous 3D scan-matching with a spinning 2D laser. In *2009 IEEE International Conference on Robotics and Automation (ICRA)* (pp. 4312-4319).

Britton, N., Yoshida, K., Walker, J., Nagatani, K., Taylor, G., & Dauphin, L. (2015). Lunar micro rover design for exploration through virtual reality tele-operation, *Field and Service Robotics* (259–272). Springer

Cole, D. M., & Newman, P. M. (2006). Using laser range data for 3D SLAM in outdoor environments. In: *2006 IEEE International Conference on Robotics and Automation (ICRA)* (pp. 1556-1563)

Durrant-Whyte, H., & Bailey, T. (2006). Simultaneous localization and mapping: Part I. *IEEE Robotics & Automation Magazine*, *13*(2), 99–110.

Huang, A. S., Bachrach, A., Henry, P., Krainin, M., Maturana, D., Fox, D., & Roy, N. (2011). Visual odometry and mapping for autonomous flight using an RGB-D camera., 1-16.

Huntsberger, T., Stroupe, A., Aghazarian, H., Garrett, M., Younse, P., & Powell, M. (2007). TRESSA: Teamed robots for exploration and science on steep areas. *Journal of Field Robotics*, *24*(11–12), 1015–1031.

Kubelka, V., Oswald, L., Pomerleau, F., Colas, F., Svoboda, T., & Reinstein, M. (2015). Robust data fusion of multimodal sensory information for mobile robots. *Journal of Field Robotics*, *32*(4), 447–473.

Matthews, J. B. & Nesnas, I. (2012). On the design of the Axel and DuAxel rovers for extreme terrain exploration, 1–10.

McGarey, P., MacTavish, K., Pomerleau, F., & Barfoot, T. D. (2017). TSLAM: Tethered simultaneous localization and mapping for mobile robots. *The International Journal of Robotics Research*, *36*(12), 1363–1386.

McGarey, P., Polzin, M., & Barfoot, T. D. (2017). Falling in line: Visual route following on extreme terrain for a tethered mobile robot.

McGarey, P., Pomerleau, F., & Barfoot, T. D. (2015). System design of a Tethered Robotic Explorer (TReX) for 3D mapping of steep terrain and harsh environments.

McGarey, P., Tang, T., Yoon, D., Pomerleau, F., & Barfoot, T. D. (2017). Field deployment of the tethered robotic explorer to map extremely steep terrain.

Nagatani, K., Kiribayashi, S., Okada, Y., Otake, K., Yoshida, K., Tadokoro, S., & Kawatsuma, S. (2013). Emergency response to the nuclear accident at the Fukushima Daiichi Nuclear Power Plants using mobile rescue robots. *Journal of Field Robotics*, *30*(1), 44–63.

Osinski, G. R., Barfoot, T. D., Ghafoor, N., Izawa, M., Banerjee, N., Jasiobedzki, P., & Flemming, R. (2010). Lidar and the mobile scene modeler (mSM) as scientific tools for planetary exploration. *Planetary and Space Science*, *58*(4), 691–700.

Pomerleau, F., Colas, F., Siegwart, R., & Magnenat, S. (2013). Comparing ICP variants on real-world data sets. *Autonomous Robots*, *34*(3), 133–148.

Sinden, F. (1990). The tethered robot problem. *The International Journal of Robotics Research*, *9*(1), 122–133.

Smith, R., Self, M., & Cheeseman, P. (1990). Estimating uncertain spatial relationships in robotics, *Autonomous Robot Vehicles* (167–193). Springer

Stenning, B., Bajin, L., Robson, C., Peretroukhin, V., Osinski, G. R., & Barfoot, T. D. (2015). Towards autonomous mobile robots for the exploration of steep terrain, *Field and Service Robotics* (33–47). Springer

Tang, T. Y., Yoon, D. J., Pomerleau, F., & Barfoot, T. D. (2018). Learning a bias correction for lidar-only motion estimation.

Teshnizi, R. H. & Shell, D. (2014). Computing cell-based decompositions dynamically for planning motions of tethered robots., 6130-6135.

Wettergreen, D., Thorpe, C., & Whittaker, R. (1993). Exploring Mount Erebus by walking robot. *Robotics and Autonomous Systems*, *11*(3), 171–185.

Zhang, J., & Singh, S. (2014). LOAM: Lidar odometry and mapping in real-time. In: *Robotics: Science and Systems Conference (RSS)* (pp. 109-111).

Zhang, J., & Singh, S. (2015). Visual-lidar odometry and mapping: Low-drift, robust, and fast. In: *2015 IEEE Interenational Conference on Robotics and Automation (ICRA)* (pp. 2174–2181).

How to cite this article: McGarey P, Yoon D, Tang T, Pomerleau F, Barfoot TD. Developing and deploying a tethered robot to map extremely steep terrain. *J Field Robotics*. 2018;35:1327–1341. https://doi.org/10.1002/rob.21813